Synthetic strategy toward ineleganolide: A cautionary tale

Alexander Q. Cusumano, K.N. Houk, Brian M. Stoltz

PII: S0040-4020(21)00511-1

DOI: https://doi.org/10.1016/j.tet.2021.132289

Reference: TET 132289

To appear in: *Tetrahedron*

Received Date: 2 May 2021

Revised Date: 10 June 2021

Accepted Date: 10 June 2021

Please cite this article as: Cusumano AQ, Houk KN, Stoltz BM, Synthetic strategy toward ineleganolide: A cautionary tale, *Tetrahedron*, https://doi.org/10.1016/j.tet.2021.132289.

Graphical Abstract

To create your abstract, type over the instructions in the template box below.
Fonts or abstract dimensions should not be changed or altered.

Synthetic strategy toward ineleganolide: A cautionary tale.

Leave this area blank for abstract info.

Alexander Q. Cusumano [a], *K. N. Houk* [b,*], *Brian M. Stoltz* [a,*]

[a] *Division of Chemistry and Chemical Engineering, California Institute of Technology, Pasadena, CA 91125, USA*

[b] *Department of Chemistry and Biochemistry, University of California, Los Angeles, California 90095, USA*

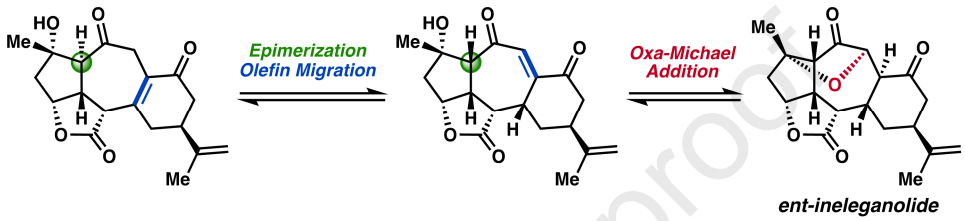

Tetrahedron
journal homepage: www.elsevier.com

Synthetic strategy toward ineleganolide: A cautionary tale.

Alexander Q. Cusumano [a], K. N. Houk [b,*], Brian M. Stoltz [a,*]

[a] Division of Chemistry and Chemical Engineering, California Institute of Technology, Pasadena, California 91125, USA
[b] Department of Chemistry and Biochemistry, University of California, Los Angeles, California 90095, USA

ARTICLE INFO

Article history:
Received
Received in revised form
Accepted
Available online

Keywords:
Keyword_1
Keyword_2
Keyword_3
Keyword_4
Keyword_5

ABSTRACT

We present a case study to demonstrate how complex molecule synthesis can benefit from quantum mechanics (QM) calculations. Theory is applied in two contexts: testing the chemical intuition used in retrosynthetic planning, along with expediting the resolution of unexpected challenges encountered during the course of the synthesis. From a computational lens, we examine retrospectively the strategies employed and the decisions made during our synthetic efforts toward the diterpenoid natural product ineleganolide. Seemingly logical and robust hypotheses are found to be ill-fated after theoretical investigation. Prior knowledge of these issues may have potentially saved valuable time and resources during our synthetic efforts. This cautionary tale suggests that synthetic campaigns can benefit from computational evaluation of synthetic plans.

1. Introduction

The polycyclic furanobutenolide-derived norcembranoid diterpeniod family of natural products presents a significant synthetic challenge owing to their stereochemical complexity and highly oxidized frameworks.[1,2] Of the members in this class of natural products, ineleganolide (**1**) bears a particularly formidable [6–7–5–5]-tetracyclic core with a bridging dihydrofuranone (Figure 1).[3] Other isomeric species include horiolide (**2**)[4] and kavaranolide (**3**).[1d] Our group's efforts toward the synthesis of *ent*-ineleganolide (***ent*-1**) span over a decade, culminating in the successful synthesis of the tetracyclic core, as well as installation of eight of the nine stereogenic centers of the target molecule.[5] Unfortunately, our efforts to complete the synthesis by late-stage installation of the bridging dihydrofuranone were ultimately unsuccessful. In this study, we employ quantum mechanics (QM) calculations to examine the unforeseen shortcomings in our prior synthetic strategy. In doing so, we highlight how theoretical calculations aid in uncovering issues in a synthetic approach that may otherwise appear logical and robust. Namely, we investigate how theory may be applied in two strategic settings: (1) aiding in the resolution of unforeseen challenges, and (2) testing key hypotheses made in the retrosynthetic planning phase.[6]

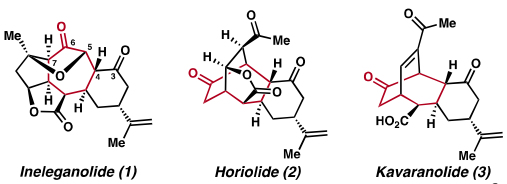

Figure 1. Representative members of the norcembranoid diterpene family of natural products.

2. Results and discussion

2.1. Installing oxidation at C(6) – An unanticipated challenge.

Our retrosynthetic analysis of *ent*-ineleganolide (***ent*-1**) began with identifying the C(5)–O bond as a key initial disconnection.[5] We envisioned the C–O bond could be forged through an intramolecular oxa-Michael addition of enedione **4**, which may be accessed from oxidation of diketone **5**. Concomitant oxidation of the C(6) position with setting of stereochemistry at C(7) would be achieved by reductive epoxide opening of **7**, followed by oxidation of the resultant secondary alcohol (**6**). Epoxide **7** was accessed in seven steps from diol **8** and *(S)*-desmethylcarvone

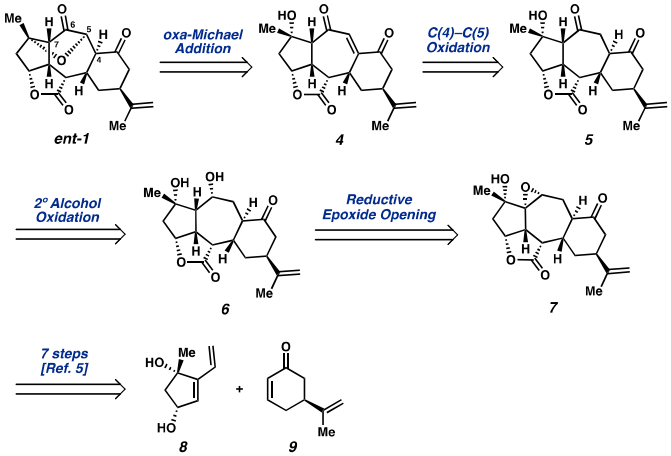

(**9**), the details of which are reported elsewhere.[5]

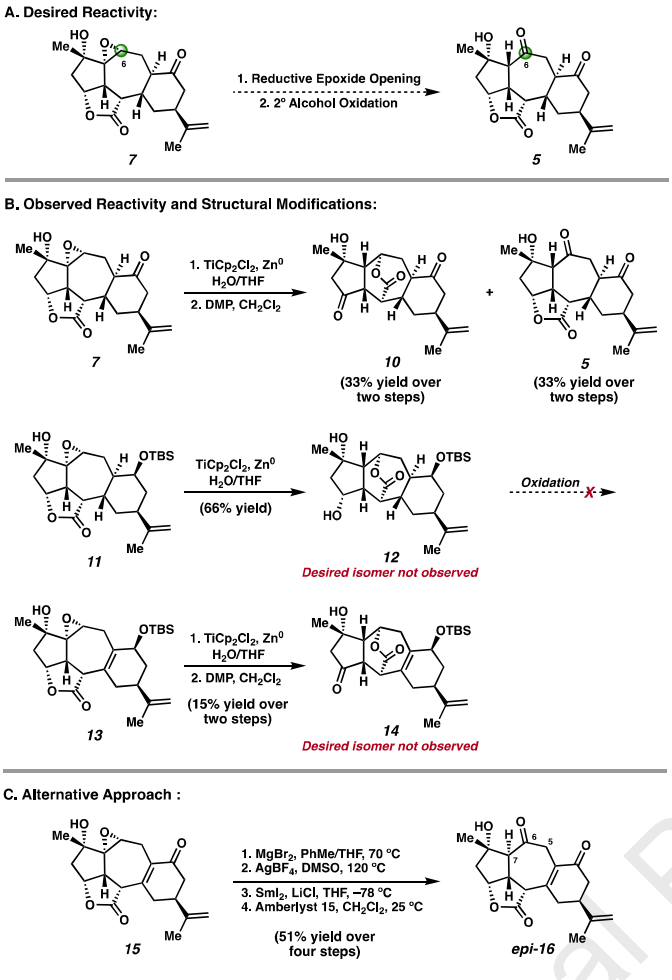

Figure 3. (A) Envisioned sequential regioselective Ti(III)-mediated reductive epoxide opening/alcohol oxidation sequence to ketone **5**. (B) Undesired translactonization of diol **6** derivatives. (C) Alternative four-step approach to enone ***epi*-16**.

Unfortunately, from epoxide **7**, installation of the C(6) ketone proved to be a challenge. Initial efforts focused on the direct conversion of epoxide **7** to the desired ketone (**5**) via a 1,2-hydride shift were unsuccessful. As such, the two-step strategy consisting of a regioselective Ti(III)-mediated reductive epoxide opening followed by oxidation of the resulting alcohol (**6**) to ketone **5** was pursued (Figure 3A). In this process, the intermediate 1,3-diol (**6**) undergoes translactonization with the C(6) hydroxyl group, affording the undesired translactonized product (**10**) in a 1:1 ratio with the desired ketone (**5**) (Figure 3B).[5d] Attempts to convert lactone **10** to ketone **5** were unsuccessful. This obstruction to material throughput at this late stage of the synthesis prompted efforts to improve the selectivity by modifying the scaffold. The C(3) ketone of **7** was reduced to the corresponding alcohol, which was then converted to the corresponding *tert*-butyldimethylsilyl (TBS) ether **11**. However, subjecting TBS ether **11** to the reductive epoxide opening conditions exclusively furnished undesired lactone **12** in 66% yield. In an effort to distance the C(6) alcohol from the γ-butyrolactone, we sought to planarize the [6,7] ring junction by preparing allylic TBS ether **13**. This strategy proved unsuccessful as translactonized product **14** was exclusively observed upon epoxide opening and subsequent oxidation. After a significant investment of time and effort, the epoxide opening/alcohol oxidation approach to the installation of the C(6) ketone was ultimately abandoned. Instead, the desired oxygenation pattern was established via a four step sequence from enone **15**, magnesium(II) bromide, concomitant Kornblum oxidation of the resultant alkyl bromide, reductive opening of the cyclic ether by *in situ* generated $SmCl_2$, and β-elimination by treatment with Amberlyst 15 resin to ultimately yield enone ***epi*-16** (Figure 3C).[5a] We note that the C(7) stereocenter of enone **16** is epimeric to that of the natural product (***ent*-1**).[5b]

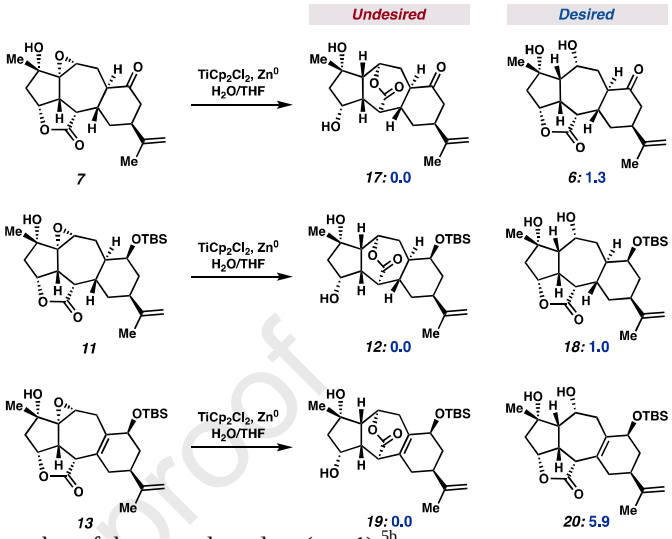

Figure 4. Comparing relative free energies (given in kcal/mol) of 1,3-diol intermediates derived from **7**, **11**, and **13**.

Given the substantial investment of time and resources required for these empirical explorations, we question whether this process may have been streamlined with the aid of computational analysis. Insights into the feasibility of a desired transformation would aid in focusing experimental efforts toward the most productive path forward. Ideally, the theoretical model employed would take the simplest form possible, while still maintaining sufficient details as to accurately capture the reactivity paradigm at hand. In generating such a model, we form a base of assumptions that will simplify and expedite the in-silico experimentation process. In the system discussed herein, we assume that (1) translactonization is relatively facile under the reaction conditions, and (2) the subsequent oxidation step is unable to sufficiently kinetically or dynamically resolve the diol product distribution. As a result, the final product distribution is approximated by the ratio of diol products from the epoxide opening step. Given these intermediates are assumed to be under thermal equilibration, the Gibbs free energies of the constitutional isomers are compared.

Geometries and thermodynamic corrections are obtained by density functional theory (DFT) calculations at the ωB97X-D3/def2-SV(P) level of theory.[7,8] Final Gibbs free energies are obtained by applying thermodynamical corrections to coupled cluster electronic energies (DLPNO-CCSD(T)/def2-TZVPP/SMD(THF)).[9,10,11] Conformational entropy is included in the reported free energies by the *mixture of components* model as formulated by DeTar.[12] Full computational details are provided in the experimental section. For a substrate to warrant adding steps in deviating from the current synthetic route, it must be predicted to significantly out-perform the 1:1 selectivity of **5**:**10** (the desired being isolated in 33% yield). Taking error into account, we suggest a derivative with a calculated preference for the desired diol of ≥ 1.0 kcal/mol to be selected as a target for synthesis.

Reexamining the aforementioned substrates, we find that none of the originally proposed deviations are predicted to favor

the product (**17**, **12**, and **19**). From epoxide **7**, undesired diol **17** is predicted to be favored over diol **6** in a 9:1 ratio (ΔG = 1.3 kcal/mol) (Figure 4). Experimentally, direct oxidation of the crude mixture delivers ketones **5** and **10** in a 1:1 isolated ratio. Without knowing the precise ratio of **17**:**6** prior to oxidation, it is challenging to quantitatively assess the resolving power of the oxidation step; however, the qualitative trends should remain useful. Similarly, from epoxides **11** and **13**, the undesired translactonized diol is predicted to be the major product (Figure 4). Considering our predetermined threshold for what is considered a target of significant interest, in retrospect, none of the proposed modifications would have been recommended for experimental investigation. Interpreting these initial results in the context of synthetic planning, two strategies moving forward would have been (1) to continue in-silico screening of alternative scaffold modifications to favor the desired ketone and suppress formation of the undesired lactone, followed by experimental verification, or (2) to recognize the difficulty in biasing the reactivity and explore alternative routes to minimize efforts in endeavors with lower probability of success. After extensive experimental efforts along the lines of the first strategy, the latter was indeed ultimately adopted.

2.2. Olefin isomerization – Key assumptions.

Above, we propose the use of theoretical calculations to facilitate decision making upon encountering unexpected challenges. However, during the course of a total synthesis, such an approach may also be adopted in the synthetic planning phase. Computational investigation allows for a quantitative assessment of the qualitative predictions derived from chemical intuition. Theoretical calculations serve to uncover instances in which these rational assumptions may, in practice, lead to counterintuitive results. An example of such discrepancy between chemical intuition and observation arose in the final C–O bond formation in the endgame of our route to ineleganolide, which ultimately impeded our efforts to complete the total synthesis.

When initially planning our synthesis, we envisioned access to enedione **4** through desaturation or epimerization and olefin isomerization of ketone **5** or enones **16**/***epi*-16**, respectively. A subsequent oxa-Michael addition to forge the C(5)–O bond would then complete the synthesis of *ent*-ineleganolide (Figure 5A). Key to both of these approaches, we hypothesized that facile isomerization of the endocyclic olefin will favor the more highly conjugated enedione **4** over its enone isomers **16**/***epi*-16**. Additionally, we assumed the natural product to be a global free energy minimum with respect to the unsaturated intermediates and that the reversible nature of the conjugate addition would thus favor the formation of *ent*-ineleganolide (***ent*-1**). However, despite our best efforts, neither enedione **4** nor *ent*-ineleganolide (***ent*-1**) were observed in attempts to directly desaturate dione **5**. As such, we turned our attention to olefin isomerization and epimerization of enone ***epi*-16**. Surprisingly, despite extensive efforts, no isomerization to the supposed thermodynamic product, nor oxa-Michael addition products were observed.

The lack of desired reactivity may arise from inaccuracy in our initial conjectures that olefin migration to enedione **4** to be thermodynamically favorable, and the natural product to be an energetic global minimum with respect to its isomeric intermediates. In order to evaluate whether theoretical calculations would have highlighted this discrepancy early in the synthetic planning phase, we sought to computationally investigate the matter. As aforementioned, we consider a set of assumptions geared to facilitating this investigation. Proton transfer and conformational isomerism are assumed to be rapid in olefin isomers may be derived from their relative free energies. As the Curtin–Hammett postulate is invoked, the effective barrier height for C–O bond formation must be calculated from the global minimum of the starting olefin isomers, regardless of the conformer of the reactive isomer (**4**). As previously mentioned, geometries are obtained by DFT (ωB97X-D3/def2-SV(P)).[7,8] Thermodynamical corrections obtained at the optimization level of theory, along with solvation free energies[10], are applied to coupled cluster electronic energies (DLPNO-CCSD(T)/def2-TZVPP). Due to the computational cost of the latter, coupled with the large number of conformers for each intermediate, pre-screening with DFT (ωB97M-V/def2-

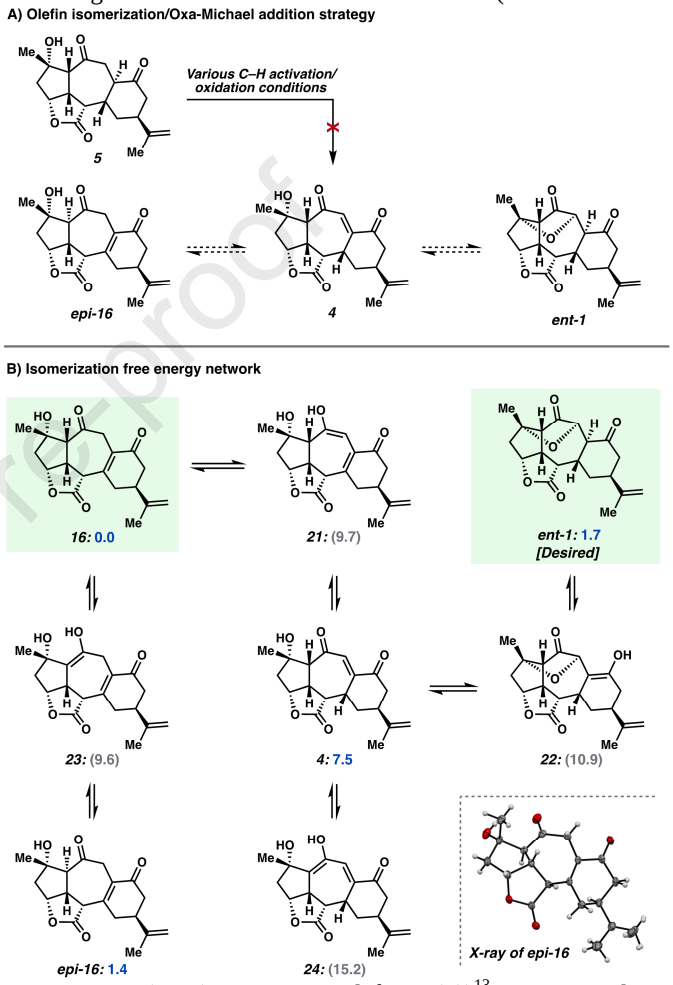

TZVPP/SMD(THF)//ωB97X-D3/def2-SV(P))[13] was carried out to identify which isomers are of energetic relevance to be treated with the DLPNO-CCSD(T) description. Full details on the computational methodologies employed are provided in the experimental section.

Figure 5. (A) End game strategy for the completion of the synthesis of *ent*-ineleganolide (***ent*-1**) from either **5** or ***epi*-16**. (B) Relative free energies (in kcal/mol) between key intermediates in the isomerization from ***epi*-16** to ***ent*-1**. For high energy intermediates not treated by DLPNO-CCSD(T), relative free energies from DFT are given in parentheses.

In considering epimerization/isomerization from enone ***epi*-16** to enedione **4** and to *ent*-ineleganolide (***ent*-1**), the requisite enol tautomers (**21**, **22**, and **23**) for their interconversions are also modeled (Figure 5B). The C(7) enol tautomer of **4** (**24**) was also considered. We note the trans-fused [5,7] enedione isomer of **4** is unable to undergo productive C–O bond formation due to geometric constraints. Based on current results, the intermediate would likely be high in energy, and hence is excluded.

24) to be significantly higher in energy than their ketone precursors. As such, coupled cluster energies are obtained for intermediates **16**, **epi-16**, **4**, and *ent*-ineleganolide (***ent*-1**). Surprisingly, *ent*-ineleganolide (***ent*-1**) is not found to be the global free energy minimum along the isomerization free energy surface. In fact, the Boltzmann-weighted populations derived from the relative free energies of the low energy conformers for compounds ***ent*-1**, **16**, ***epi*-16**, and **4**, reveals an equilibrated product distribution of < 5% *ent*-ineleganolide (***ent*-1**), 87% enone **16**, 8% enone ***epi*-16**, and < 0.1% enedione **4**. In accord with the coupled cluster calculations, DFT (ωB97M-V) calculations predict an energetic preference of 1.1 kcal/mol for **16** over ***ent*-1**. The computational analysis reveals two fallacies within our initial chemical intuition-derived assumptions. First, we find olefin migration of enone ***epi*-16** to enedione **4** is not thermodynamically favorable. Enedione **4** is 7.5 and 6.1 kcal/mol higher in energy than enones ***epi*-16** and **16**, respectively. Second, *ent*-ineleganolide (***ent*-1**) is not the global thermodynamic well as anticipated. Upon equilibration of the system, the natural product comprises less than 5 mol % of the partitioned intermediates. While the precise numerical values for the maximum yield are anticipated to be solvent/temperature dependent, this simple analysis highlights a deeper underlying challenge to the synthetic strategy as a whole.

Although only considering minima on the free energy surface, the significant thermodynamical preference for enone **16** over the reactive enedione isomer (**4**) does bear consequences on the kinetic accessibility of *ent*-ineleganolide (***ent*-1**). Under equilibrating conditions, the apparent barrier height to C–O bond formation is an additional 7.5 kcal/mol higher than the barrier to C–O bond formation directly from enedione **4**. Hence, in order to achieve equilibrium between **16** (or ***epi*-16**) and ***ent*-1**, the isolated C–O bond forming event would have to be relatively facile, ideally with a barrier of less than 15 kcal/mol relative to **4**, to maintain a reasonable rate at ambient temperature. Moreover, given that *ent*-ineleganolide (***ent*-1**) is not a global minimum, yet is still able to be isolated, the barrier to C–O bond formation/breaking in the absence of exogenous strong acid/base catalyst is anticipated to be intractably high at ambient temperatures. This conjecture may be tested experimentally by subjecting an authentic sample of ineleganolide to increasingly forcing conditions and monitoring for transformation to enones **16** and ***epi*-16**. Biosynthetically, the C(5)–O bond is thought to be formed at an early stage and introduced as a 3(2H)-furanone moiety.[2b] Lastly, we note that if keto/enol tautomerization is rapid relative to other bond forming processes, then the preceding strategy of direct desaturation of diketone **5** to enone **4** would have also succumbed to these issues.

In summary, these findings suggest the original olefin migration/oxa-Michael addition strategy to forge the C(5)–O bond of ineleganolide to be precarious. Checking known assumptions in the early stages of synthetic planning would have revealed the shortcomings behind what otherwise would appear to be a robust strategy. Alternative disconnections could then be considered, perhaps with special attention focused on the problematic C(5)–O bond.

3. Conclusions

We present a case study in which the utility of theoretical calculations is demonstrated in the context of our efforts in the synthesis of the norcembranoid diterpenoid natural product ineleganolide. Computational investigations are applied to two distinct challenges. First, theory is applied in a situation in which the installation of oxidation at the C(6) position of late-stage intermediate **7**. Several structural modifications were proposed to alleviate the deleterious trans-lactonization occurring after reductive epoxide opening. Without a method to evaluate the efficacy of the proposals, each compound had to be synthesized in order to be verified experimentally. Unfortunately, all approaches were unfruitful in mitigating the undesired reactivity. A simplified computational model for predicting the success of each proposal is developed. With this approach, we find that none of the proposed modifications are predicted to be within the tolerances to be considered as warranting experimental investigation. Hence, we imagine that theoretical calculations may have proven useful in minimizing time and experimental effort sacrificed to these efforts. Second, we utilize computational investigation to evaluate assumptions that are made in the retrosynthetic planning phase of the synthesis. Despite extensive experimental efforts, the olefin migration/oxa-Michael addition cascade in the last step of the synthesis was never realized. Our calculations suggest the equilibrating approach to be ill-fated by virtue of the thermodynamical relationship between the natural product and its isomeric forms. These initially counterintuitive observations, and the resulting fallacy in the strategy, may have been highlighted sooner with the aid of theory. In summary, experimentation provides the ultimate determination of success or failure; however, we highlight how calculations can contribute to refining plans for total synthesis.

4. Experimental section

4.1. Computational Details

All quantum mechanical calculations were carried out with the ORCA program.[14] Geometry optimizations and harmonic frequency calculations were carried out with density functional theory (DFT) in the gas phase. The dispersion-corrected, range-separated hybrid functional ωB97X-D3 was employed with the def2-SV(P) basis set on all atoms.[7,8] Final solvated DFT electronic energies were obtained with the ωB97M-V functional[13] paired with the def2-TZVPP basis set[8] on all atoms and SMD model[10] for implicit solvation for THF. Domain based local pair natural orbital (DLPNO) CCSD(T) single point calculations are used throughout this investigation.[9] These calculations are carried out in the gas phase, employing the def2-TZVPP basis and NormalPNO parameter cutoffs as implemented in the ORCA program. To obtain the final "solvated" coupled-cluster electronic energies, free energy of solvation (ΔG_{solv}) calculated with DFT at the ωB97M-V/def2-TZVPP/SMD(THF) level of theory were added to the gas phase DLPNO-CCSD(T) electronic energies. To these solvation-corrected coupled cluster electronic energies are added thermal and entropic corrections obtained from harmonic frequency calculations at the optimization level of theory. The quasi-rigid rotor harmonic oscillator approach is applied to correct for the breakdown of the harmonic oscillator approximation at low vibrational frequencies.[15] Translational and rotational entropies obtained by the ideal gas treatment are scaled by a factor of 0.5.[16] Conformational entropy arising from multiple low energy thermally populated conformers is taken into account by the *mixture of components* model of DeTar.[12] A correction to the entropy (S_{conf}) is computed as the average relative entropies of the conformers (S_{avg}) plus a mixing entropy (S_{mix}). S_i is the relative entropy of the i^{th} conformer, χ_i is its mole fraction based on free energies.

$$S_{conf} = S_{avg} + S_{mix}$$

$$S_{mix} = -R\sum \chi_i \ln(\chi_i)$$

Finally, correcting for a 1 M standard state affords the final Gibbs free energies:

$$G^{*}_{final} = E^{CC}_{el} + ZPE + E_{therm} - T\left(S_{vib} + S_{conf} + 0.5(S_{trans} + S_{rot})\right) + \Delta G^{DFT}_{solv} + \Delta G^{0\rightarrow *}$$

The RI and chain-of-spheres (COS)[17] approximations were used for Coulomb and exchange integrals, respectively, where applicable (keyword "RIJCOSX"), paired with the def2/J Coulomb fitting basis.[18] Tight grid settings were employed (keywords "Grid6 NoFinalGrid GridX7" for coupled cluster calculations; "Grid7 NoFinalGrid GridX9 vdwGrid5" for calculations with ωB97M-V; "Grid5 NoFinalGrid GridX7" for calculations with ωB97X-D3). Conformer searching with MMFF is carried out in Spartan Student Ver. 7.

Acknowledgments

We thank the NIH (R01 GM080269) and Caltech for financial support. The Caltech High Performance Computing (HPC) center is acknowledged for support of computational resources. This article is dedicated to Prof. Dale L. Boger.

References and notes

1. (References provided below after final section break)

Supplementary Material

An excel file with all calculated values and a zip folder with optimized structures (.xyz files) are included.

[1] (a) Li, Y.; Pattenden, G. Novel Macrocyclic and Polycyclic Norcembranoid Diterpenes from Sinularia Species of Soft Coral: Structural Relationships and Biosynthetic Speculations. *Nat. Prod. Rep.* **2011**, *28* (2), 429–440. (b) Huang, C.-Y.; Tseng, Y.-J.; Chokkalingam, U.; Hwang, T.-L.; Hsu, C.-H.; Dai, C.-F.; Sung, P.-J.; Sheu, J.-H. Bioactive Isoprenoid-Derived Natural Products from a Dongsha Atoll Soft Coral *Sinularia Erecta*. *J. Nat. Prod.* **2016**, *79* (5), 1339–1346. (c) Hegazy, M.-E. F.; Mohamed, T. A.; Elshamy, A. I.; Al-Hammady, M. A.; Ohta, S.; Paré, P. W. Casbane Diterpenes from Red Sea Coral Sinularia Polydactyla. *Molecules* **2016**, *21* (3), 308. (d) Lillsunde, K.-E.; Festa, C.; Adel, H.; De Marino, S.; Lombardi, V.; Tilvi, S.; Nawrot, D. A.; Zampella, A.; D'Souza, L.; D'Auria, M. V.; Tammela, P. Bioactive Cembrane Derivatives from the Indian Ocean Soft Coral, Sinularia Kavarattiensis. *Marine Drugs* **2014**, *12* (7), 4045–4068. (e) Thao, N. P.; Nam, N. H.; Cuong, N. X.; Quang, T. H.; Tung, P. T.; Dat, L. D.; Chae, D.; Kim, S.; Koh, Y.-S.; Kiem, P. V.; Minh, C. V.; Kim, Y. H. Anti-Inflammatory Norditerpenoids from the Soft Coral Sinularia Maxima. *Bioorg. Med. Chem. Lett.* **2013**, *23* (1), 228–231. (f) Ahmed, A. F.; Shiue, R.-T.; Wang, G.-H.; Dai, C.-F.; Kuo, Y.-H.; Sheu, J.-H. Five Novel Norcembranoids from Sinularia Leptoclados and S. Parva. *Tetrahedron* **2003**, *59* (37), 7337–7344. (g) Sheu, J.-H.; Ahmed, A. F.; Shiue, R.-T.; Dai, C.-F.; Kuo, Y.-H. Scabrolides A−D, Four New Norditerpenoids Isolated from the Soft Coral *Sinularia s Cabra*. *J. Nat. Prod.* **2002**, *65* (12), 1904–1908.

[2] (a) Horn, E. J.; Silverston, J. S.; Vanderwal, C. D. A Failed Late-Stage Epimerization Thwarts an Approach to Ineleganolide. *J. Org. Chem.* **2016**, *81* (5), 1819–1838. (b) Li, Y.; Pattenden, G. Biomimetic Syntheses of Ineleganolide and Sinulochmodin C from 5-Episinuleptolide via Sequences of Transannular Michael Reactions. *Tetrahedron* **2011**, *67* (51), 10045–10052.

[3] Duh, C.-Y.; Wang, S.-K.; Chia, M.-C.; Chiang, M. Y. A Novel Cytotoxic Norditerpenoid from the Formosan Soft Coral Sinularia Inelegans. *Tetrahedron Letters* **1999**, *40* (33), 6033–6035.

[4] Radhika, P.; Subba Rao, P. V.; Anjaneyulu, V.; Asolkar, R. N.; Laatsch, H. Horiolide, a Novel Norditerpenoid from Indian Ocean Soft Coral of the Genus *Sinularia*. *J. Nat. Prod.* **2002**, *65* (5), 737–739.

[5] (a) Robert A. Craig, I. I.; Roizen, J. L.; Smith, R. C.; Jones, A. C.; Virgil, S. C.; Stoltz, B. M. Enantioselective, Convergent Synthesis of the Ineleganolide Core by a Tandem Annulation Cascade. *Chem. Sci.* **2016**, *8* (1), 507–514. (b) Craig, R. A.; Roizen, J. L.; Smith, R. C.; Jones, A. C.; Virgil, S. C.; Stoltz, B. M. Correction: Enantioselective, Convergent Synthesis of the Ineleganolide Core by a Tandem Annulation Cascade. *Chem. Sci.* **2019**, *10* (4), 1254–1255. (c) Roizen, J. L.; Jones, A. C.; Smith, R. C.; Virgil, S. C.; Stoltz, B. M. Model Studies To Access the [6,7,5,5]-Core of Ineleganolide Using Tandem Translactonization–Cope or Cyclopropanation–Cope Rearrangements as Key Steps. *J. Org. Chem.* **2017**, *82* (24), 13051–13067. (d) Craig, R. A.; Smith, R. C.; Roizen, J. L.; Jones, A. C.; Virgil, S. C.; Stoltz, B. M. Unified Enantioselective, Convergent Synthetic Approach toward the Furanobutenolide-Derived Polycyclic Norcembranoid Diterpenes: Synthesis of a Series of Ineleganoloids by Oxidation-State Manipulation of the Carbocyclic Core. *J. Org. Chem.* **2019**, *84* (12), 7722–7746.

[6] For examples of computational chemistry in the context of total synthesis, see the following references and the references therein: (a) Elkin, M.; Newhouse, T. R. Computational Chemistry Strategies in Natural Product Synthesis. *Chem. Soc. Rev.* **2018**, *47* (21), 7830–7844. (b) Schuppe, A. W.; Liu, Y.; Newhouse, T. R. An Invocation for Computational Evaluation of Isomerization Transforms: Cationic Skeletal Reorganizations as a Case Study. *Nat. Prod. Rep.* **2021**, *38* (3), 510–527.

[7] Lin, Y.-S.; Li, G.-D.; Mao, S.-P.; Chai, J.-D. Long-Range Corrected Hybrid Density Functionals with Improved Dispersion Corrections. *J. Chem. Theory Comput.* **2013**, *9* (1), 263–272.

[8] Weigend, F.; Ahlrichs, R. Balanced Basis Sets of Split Valence, Triple Zeta Valence and Quadruple Zeta Valence Quality for H to Rn: Design and Assessment of Accuracy. *Phys. Chem. Chem. Phys.* **2005**, *7* (18), 3297–3305.

[9] (a) Riplinger, C.; Neese, F. An Efficient and near Linear Scaling Pair Natural Orbital Based Local Coupled Cluster Method. *J. Chem. Phys.* **2013**, *138* (3), 034106. (b) Riplinger, C.; Sandhoefer, B.; Hansen, A.; Neese, F. Natural Triple Excitations in Local Coupled Cluster Calculations with Pair Natural Orbitals. *J. Chem. Phys.* **2013**, *139* (13), 134101. (c) Riplinger, C.; Pinski, P.; Becker, U.; Valeev, E. F.; Neese, F. Sparse Maps—A Systematic Infrastructure for Reduced-Scaling Electronic Structure Methods. II. Linear Scaling Domain Based Pair Natural Orbital Coupled Cluster Theory. *J. Chem. Phys.* **2016**, *144* (2), 024109.

[10] Note that for final electronic energies evaluated at the DLPNO-CCSD(T) level of theory, single point calculations are carried out in the gas phase. Solvation free energy is calculated at the DFT level (ωB97M-V/def2-TZVPP/SMD(THF)) and added to the gas phase coupled cluster electronic energies. For SMD implicit solvation, see: Marenich, A. V.; Cramer, C. J.; Truhlar, D. G. Universal Solvation Model Based on Solute Electron Density and on a Continuum Model of the Solvent Defined by the Bulk Dielectric Constant and Atomic Surface Tensions. *J. Phys. Chem. B* **2009**, *113* (18), 6378–6396.

[11] (a) Liakos, D. G.; Sparta, M.; Kesharwani, M. K.; Martin, J. M. L.; Neese, F. Exploring the Accuracy Limits of Local Pair Natural Orbital Coupled-Cluster Theory. *J. Chem. Theory Comput.* **2015**, *11* (4), 1525–1539. (b) Liakos, D. G.; Neese, F. Is It Possible To Obtain Coupled Cluster Quality Energies at near Density Functional Theory Cost? Domain-Based Local Pair Natural Orbital Coupled Cluster vs Modern Density Functional Theory. *J. Chem. Theory Comput.* **2015**, *11* (9), 4054–4063. (c) Liakos, D. G.; Guo, Y.; Neese, F. Comprehensive Benchmark Results for the Domain Based Local Pair Natural Orbital Coupled Cluster Method (DLPNO-CCSD(T)) for Closed- and Open-Shell Systems. *J. Phys. Chem. A* **2020**, *124* (1), 90–100.

[12] (a) DeTar, D. F. Theoretical Ab Initio Calculation of Entropy, Heat Capacity, and Heat Content. *J. Phys. Chem. A* **1998**, *102* (26), 5128–5141. See also: (b) Guthrie, J. P. Use of DFT Methods for the Calculation of the Entropy of Gas Phase Organic Molecules: An Examination of the Quality of Results from a Simple Approach. *J. Phys. Chem. A* **2001**, *105* (37), 8495–8499.

[13] Mardirossian, N.; Head-Gordon, M. *ω*B97M-V: A Combinatorially Optimized, Range-Separated Hybrid, Meta-GGA Density Functional with VV10 Nonlocal Correlation. *J. Chem. Phys.* **2016**, *144* (21), 214110.

[14] (a) Neese, F. Software Update: The ORCA Program System, Version 4.0. *Wiley Interdiscip. Rev.: Comput. Mol. Sci.* **2018,** *8*, No. e1327. (b) Neese, F. The ORCA Program System. *Wiley Interdiscip. Rev.: Comput. Mol. Sci.* **2012**, *2*, 73−78.

[15] Grimme, S. Supramolecular Binding Thermodynamics by Dispersion-Corrected Density Functional Theory. *Chemistry – A European Journal* **2012**, *18* (32), 9955–9964.

[16] (a) Izato, Y.; Matsugi, A.; Koshi, M.; Miyake, A. A Simple Heuristic Approach to Estimate the Thermochemistry of Condensed-Phase Molecules Based on the Polarizable Continuum Model. *Phys. Chem. Chem. Phys.* **2019**, *21* (35), 18920–18929. (b) Finkelstein, A. V.; Janin, J. The Price of Lost Freedom: Entropy of Bimolecular Complex Formation. *Protein Engineering, Design and Selection* **1989**, *3* (1), 1–3.

[17] Neese, F.; Wennmohs, F.; Hansen, A.; Becker, U. Efficient, Approximate and Parallel Hartree-Fock and Hybrid DFT Calculations. A 'Chain-of-Spheres' Algorithm for the Hartree-Fock Exchange. *Chemical Physics* **2009**, *356*, 98–109.

[18] Weigend, F. Accurate Coulomb-Fitting Basis Sets for H to Rn. *Phys. Chem. Chem. Phys.* **2006**, *8* (9), 1057–1065.

Declaration of interests

☒ The authors declare that they have no known competing financial interests or personal relationships that could have appeared to influence the work reported in this paper.

☐The authors declare the following financial interests/personal relationships which may be considered as potential competing interests: